The effect of inhibiting nuclear export on glial and fibrotic scar formation as related to wound healing during spinal cord injury in rats

Abstract:

Spinal cord injury is a devastating injury affecting between 250,000 and 500,000 people in the world every year (*Spinal Cord Injury*, 2013). It involves a primary injury and complex secondary injury. After injury the glial and fibrotic scar form and have important protective effects but contribute to an environment that prevents axonal regeneration. The impactful and multifaceted roles of the scars after spinal cord injury causes them to be good targets for treatments for spinal cord injury. In this paper, I explore the effect of inhibiting nuclear export by exportin 1 on expression levels of various genes involved in glial and fibrotic scarring. Here I show that in this preliminary experiment inhibiting exportin 1 does not cause significant changes in the mRNA expression levels of *Yap*, *Taz*, *P27*, or *Pdgfrb*.

I. Introduction

Injuries to the spinal cord can be extremely severe. These traumatic injuries can cause chronic disabilities including paralysis and loss of motor and sensory functions. A spinal cord injury consists of a primary and secondary phase. The primary phase is the injury itself due to a physical force such as a motor vehicle accident, or a high fall (*Spinal Cord Injury*, 2023). The direct damage from the primary injury leads to the secondary injury.

The secondary injury is a cascade consisting of many processes and occurring over a long period of time (Hellenbrand et al., 2021). The injury causes cell death of both neurons and glial cells through apoptosis and necrosis (Shi et al., 2021). In addition, axons are de-myelinated and reactive oxygen species released by immune cells cause damage. The extracellular matrix deposition and the environment after injury prevents axonal regeneration (Perez-Gianmarco & Kukley, 2023). The secondary injury also involves immune cells such as macrophages, microglia, T-cells, and neutrophils rushing to the site of injury. The immune cells migrate to the injury site to clean up debris, but they also lead to inflammation and obstruct healing.

After immune cells have migrated to the lesion site, glial cells will proliferate and begin gliosis, forming the glial scar. The glial scar is made up of astrocytes which surround the lesion site. This contains the immune cells, preventing them from reaching beyond the lesion site and causing further damage. This gives the glial scar a protective effect. However, the glial scar is also involved in a change in the extracellular matrix, leading to an inhibitory environment to axonal regeneration (Perez-Gianmarco & Kukley, 2023).

The fibrotic scar functions together with the glial scar to form a barrier and contain immune cells (Li et al., 2021). Macrophages secrete profibrotic cytokines to cause fibroblasts to migrate to the injury site where they form the fibrotic scar inside the lesion. They produce extracellular matrix proteins that lead to scar formation (Ayazi et al., 2022). Most fibroblasts involved in fibrosis come from pericytes (Yao et al., 2022; Li et al., 2021). The scar formed as a result of these cells can block axonal regeneration, both physically and with inhibitory molecules such as phosphacan, neural glial antigen 2, tenascin-C, and semaphorin III (Ayazi et al., 2022). However, the fibrotic scar also has an important role in protection after injury. The fibrotic scar is important in preserving tissue integrity and sealing the injury site (Ayazi et al., 2022; Li et al., 2021).

During the formation of the glial scar, astrocytes proliferate and are recruited to the lesion site due to regulatory proteins, such as YAP and the proteins it interacts with: TAZ, and p27/CDKN1B. These proteins regulate gene expression involved with astrocyte proliferation. The expression of *Yap* in astrocytes increases after spinal cord injury. If *Yap* is knocked out the formation of the glial scar is

impaired and there is less axonal regeneration due to an increase in the inflammation process (Xie et al., 2020). Therefore, YAP is very important in glial scar formation.

Additionally, YAP and TAZ work to promote fibrosis (Talbott et al., 2022). The signaling pathway in which YAP and TAZ regulate gene expression leads to increased fibrosis (Mia & Singh, 2022). PDGFRB is another protein that is involved in fibrosis, as PDGF binding to its receptor, PDGFRB, leads to the proliferation, activation, and migration of cells involved in fibrosis. *Pdgfrb* expression levels increase as fibrosis increases (Ayazi et al., 2022).

The many complex processes after spinal cord injury, including scar formation, involve a multitude of proteins. These proteins may function in the nucleus or in the cytoplasm of a cell, so the export of proteins out of the nucleus is an influential process. Whether certain proteins are exported can prevent them from functioning or allow them to function. The export of many proteins is done by exportin 1 (XPO), a nuclear export protein (Hutten & Kehlenbach, 2007). Inhibiting XPO can regulate processes involved in spinal cord injury by stopping nuclear export, leading to a possible positive effect on recovery after injury.

In this paper, I explore the effect of inhibiting nuclear export on glial and fibrotic scar formation. This is done by measuring the expression levels of several genes involved in these processes using spinal cord tissue samples from injured rats. The levels of gene expression from the spinal cord of rats given a spinal cord injury and treated with a drug to inhibit XPO is compared to levels from rats given a placebo. The genes studied are Yes Associated protein (*Yap*), Tafazzin (*Taz*), cyclin-dependent kinase inhibitor 1b (*P27*/CDKN1B), and platelet derived growth factor receptor beta (*Pdgfrb*).

When YAP leaves the nucleus it is phosphorylated and cannot function (Xie et al., 2020). Inhibiting XPO will prevent YAP from leaving the nucleus, as YAP is a ligand of XPO1, and allow it to continually function. The many proteins affected by inhibiting XPO may cause a change in *yap* expression as well. Therefore, I expect to see a change in *Yap* expression and evidence of its activity (as seen through *P27*/CDKN1B expression levels) due to the inhibiting nuclear export.

TAZ works together with YAP to promote fibrosis and as a transcriptional regulator involved in proliferation of astrocytes (Totaro et al., 2018; Talbott et al., 2022). It also functions when it is in the nucleus and dephosphorylated (Meng et al., 2016). With nuclear export inhibited, TAZ should also be able to stay in the nucleus and continually function. Therefore, I anticipate that *Taz* expression will also differ due to treatment.

YAP leads to a decrease in the expression of *P27*. This decrease in *P27* causes bFGF-induced proliferation, allowing for the proliferation of astrocytes (Xie et al., 2020). Therefore, with YAP able to continually function due to the inhibition of nuclear export, I expect to see a decrease in *P27* expression levels.

Pdgfrb is a marker of fibrosis, as it is expressed by fibroblasts and increases in expression when the fibrotic scar forms (Ayazi et al., 2022) (Li et al., 2021). However, *Pdgfrb* is also expressed in several other cell types such as endothelial cells and pericytes, so it is not a specific marker. There is not a specific marker for fibrosis available (Talbott et al., 2022). A change in *Pdgfrb* expression will correlate with a change in the fibrotic scar. I anticipate a change in expression of *Pdgfrb* due to treatment, displaying a change in the fibrotic scar.

Due to the accumulation of many proteins in the nucleus, the changes in expression of *Yap, Taz, P27*/CDKN1B, and *Pdgfrb* may be unforeseeable. The approximately 220 proteins exported by Exportin 1 will accumulate in the nucleus, affecting gene expression and may change the expression of the genes studied (Parikh et al., 2014). XPO 1 normally exports YAP, TAZ, and p27 proteins, which are all

involved in glial and fibrotic scar formation after spinal cord injury. Additionally, PDGFRB is a marker of fibrosis. In this study, I assessed the impact of XPO1 inhibition on the expression of *Yap, Taz, P27,* and *Pdgfrb* at the mRNA level.

Changes in the expression of these genes would show changes in the formation of the glial and fibrotic scar due to an inhibiting nuclear export, which would have implications in its effect on recovery after spinal cord injury. Inhibiting nuclear export has the potential to cause improved healing after spinal cord injury as the glial scar and fibrotic scar change, as shown by changes in proteins involved in these scars. The hypothesis being tested is that inhibiting XPO will regulate the mRNA levels of genes in the *Yap* pathway after spinal cord injury. This study will help clarify the effect of inhibiting XPO on the process of glial and fibrotic scar formation in relation to *Yap, Taz, P27,* and *Pdgfrb*. RT-qPCR is used to measure gene expression levels of the aforementioned genes in rats with and without spinal cord injury and with and without inhibiting XPO. A rat model is used due to its similarities in processes after injury to that of humans, and the ease in which data can be collected using a rat model (Kjell 2016).

II. Methodology:

II.a. Tissue:

Spinal cord was obtained from related experiments by Hill lab. Rats with a thoracic vertebral level 9 injury were given placebo, low dose, or high dose of drug by oral gavage, starting 2 hours after the injury and then at 1 dpi, 2 dpi, 3 dpi, 7 dpi, and 14 dpi. The rats were then sacrificed at time points of 1 dpi, 3 dpi, 7 dpi, and 14 dpi.

II.b. Primer design:

The mRNA sequences of the genes of interest (*Yap, Taz, P27,* and *Pdgfrb*), and the reference genes (*Hprt*, *Rplp1*, and *Eif2b2)*, were found on the Refseq representative rat genome database. Primer-BLAST was then used to generate primers according to the following specifications: melting temperature- 65°-75° C, optimal temperature- 70° C, must span an intron-exon gap, species- Rattus norvegicus, and max target amplicon size- 250 bp. Five primer pairs were chosen from the generated primers and their specificity and e-value (a score that represents how likely a match between sequences is by chance) were checked using the BLASTn database. Horizon discovery primer analysis was used to check if any primer dimers were likely to form. Lastly, primers were edited to be near the optimal temperature, have a % guanine and cytosine between 35 and 65, avoid any dimers, and be specific to the gene of interest. The primers chosen are detailed in table 1.

Table 1.

Primer	**Purpose**	**Fw**	**Rv**	**Concentration (nM)**	**Efficiency**	**Amplification factor**
Hprt	Reference gene	CTCATGGACTGATTATGGACAGGAC	GCAGGTCAGCAAAGAACTTATAGCC	400	108%	2.08
Rplp1	Reference gene	AAAGCAGCTGGTGTCAATGTT	GCAGATGAGGCTTCCAATGT	800	105.96%	2.06
Eif2b2	Reference gene	ATCCGCAGAGAGGGTAGGAG	GTGCCTTCCAGTTCCACTAGC	500	106%	2.06

Taz	Yap pathway	ACCTGAAGTTGATGC GTTGGACCCCAGC	CAAAGCGGGGGAA GTAGGGTGGACTGT	1000	106%	2.06
Yap	Yap pathway	ATCCCAGCACAGCAA ATGCTCCA	GCTCTGGCTGATGG TGTCTCCTGT	900	103%	2.04
P27	Yap pathway	GGTGCCTTCAATTGGG TCTC	GCTTCCTCATCCCTG GACAC	400	101%	2.01
Pdgfrb	Pericyte marker	GCCGGTGGGGCTCTC CCTACCC	GCCCACGAGGTCCG TGTAGCTGAGC	300	109%	2.09

Table 1. Primer Information: The name of each gene, its purpose, the sequence of its primer, the concentration of the primer used, and the efficiency and amplification factor of the primer.

II.c. RNA extraction and purification:

RNA was extracted from the spinal cord tissue using Tri-Reagent and the Direct-Zol kit reagents (Zymo Research). A one cm section from the epicenter was used and homogenized by sonication. After homogenization, 1 ml of Tri-Reagent per 50-100 mg of tissue was added. After sitting for 5 minutes, 200 µL of Chloroform was added. The sample was then vortexed, let sit for 3 minutes, and centrifuged (for 15 min at 12,00g at 4˚ C). Centrifugation allowed the separation of three phases. The clear top phase, consisting of RNA, was transferred to a separate tube.

The RNA then went through RNA purification. For every 50-100 mg of tissue 1 ml of 100% molecular biology grade ethanol was added to the RNA and it was put in a Zymo-Spin IICR column and centrifuged (10,000g for 30 seconds at room temperature). After moving the column to a new collection tube, 400 µL of RNA wash buffer was added and the tube with the column was centrifuged (10,00g for 30 seconds at 20C). Next, 75 µL of DNA digestion buffer and 5 µL of DNAse were combined and added, then the mixture was let sit at room temperature for 15 min. The flowthrough was discarded, then 400 µL of RNA Prewash buffer was added. The tube was centrifuged (at 10,00g for 30 seconds at room temperature). The previous steps were then repeated (discard flowthrough, add RNA Prewash buffer, and centrifuge). The column was washed with 700 µL of RNA Wash buffer, and was then centrifuged (10,00g for 30 seconds at room temperature). In a new collection tube, 50 µL DNAse/RNAse free water was added, then the tube was centrifuged (10,000g for 30 seconds at room temperature) to retrieve the RNA. Using the Nanodrop machine, the RNA obtained was quantified and its purity was verified using the A260/A280 and A260/A230 indexes that indicated the content of proteins in the sample and buffer contamination, respectively. Lastly, the RNA was stored at -80°C.

II.d. cDNA synthesis:

cDNA was synthesized from the RNA previously extracted. In order to make 20 µL of cDNA, 10 µL of diluted sample (with 2000 ng total RNA) and 10 µL of mastermix need to be made. To make 10 µL of 500 ng RNA, 500 ng is divided by the concentration of the RNA sample (ng/ul) and this volume of RNA sample is added. The remainder of the 10 µL of volume is completed by RNAse/DNAse free water. Following this, 2 µL of 10x Real time buffer, 0.8 µL 25x dNTP, 2 µL 10x Random primers, 4.2 µL RNAse/DNAse free water, and 1 µL MultiScribe Reverse Transcriptase were added. These amounts can be scaled up to make more cDNA. The mixture was added to PCR tubes and put in a Thermal Cycler using the following program: Step 1: 25°C 10 min, Step 2: 37°C 120 min, Step 3: 85°C 5 min, Step 4: 4°C

hold. Controls with the sample replaced with water (H2O control) or the reverse transcriptase replaced with water (NTC control) were also made.

II.e. RT-qPCR:

To make the master mix, Sybr Green, and RNAse/DNAse free water were combined along with the primer of interest. Sybr Green binds to double stranded DNA, so when the primer binds to the gene of interest and makes more copies of that DNA, the Sybr Green binds more. The fluorescence of Sybr Green increases when it is bound, so levels of fluorescence correspond to levels of the gene of interest. Primers were diluted in RNAse/DNAse free water to the desired concentration, and 2 μL of the diluted primer were added. Next, 10 μL Sybr Green (1x) and 6 μL of RNAse/DNAse free water were added. These amounts are scaled up based on how many wells of the PCR plate the master mix will be filling, by multiplying the amounts by the number of wells. The cDNA samples were diluted in RNAse/DNAse free water to desired concentrations of cDNA. Eighteen μL of master mix and 2 μL of diluted cDNA were added to each well of the PCR plate, following the preplanned layout. The PCR plate was spun and put into the PCR machine, set with the following protocol: Step 1: RT: 48°C 15 min hold, Step 2: Enzyme activation: 95°C 10 min hold, Step 3: Denature: 95°C 15 sec 40 cycles, Step 4: Anneal/Extend: Average temp of primers - 5°C 1 min 40 cycles, Step 5: Rest at 5°C.

II.f. Primer optimization:

Primer efficiency was assessed using a standard curve. This involves taking cDNA samples with known concentrations and diluting them to 500 μm, 100 μm, 20 μm, 4 μm, and 0.8 μm and finding the Cq value by doing RT-qPCR. The Cq values were graphed, and the slope of the line (change in Cq value/change in log of concentration) was used to find efficiency based on the following equation: $E=10^{-1/slope}$. If E is between 90 and 110%, it is an acceptable primer efficiency. In addition, the melt curve was examined. The melt curve was deemed acceptable if it had a single sharp peak. Several primer concentrations were tested for each primer. The lowest primer concentration with an acceptable efficiency and melt curve was chosen to be used.

II.g. Analysis:

For each gene of interest, the following analysis was completed. The Cqs of the triplicates for each animal were averaged and repeated if there was a standard deviation over 1.5. Then the Cq values from each experimental condition group were averaged and the standard deviation was calculated. These average Cq values were corrected using the calibration factor, which is found by subtracting a control plate and the plate of interest. The difference between the corrected control Cq value (uninjured group) and the corrected Cq value from each experimental group was calculated and the efficiency value of the primer for the gene of interest was raised to the power of this difference. This was done to determine the relative quantification, which is corrected for amplification efficiency for the primer. The relative gene expression was then found by dividing the relative quantification by the geometric mean of the relative quantification of the reference genes (*Hprt*, *Rplp1,* and *Eif2b2*) for each animal. The relative gene expression takes into account differences in overall gene expression in different animals by using reference genes that are expressed consistently despite experimental conditions. Lastly, log2 of each relative gene expression value was found. The fold change of the log2 values was graphed in a dot-plot for each gene.

II.h. Statistical analysis:

To compare the expression of *Yap, Taz, Pdgfrb,* and *P27* according to the factors of treatment and time a two-way ANOVA was run using GraphPad software. To find where the differences lay I ran a one-way ANOVA and used a Bonferroni post-hoc analysis.

III. Results:

The gene expression levels of several genes of interest related to glial and fibrotic scarring were compared between experimental conditions of placebo, low dose, and high dose over different time points after spinal cord injury using RT-qPCR testing. The changes in expression levels of *Yap, Taz, Pdgfrb,* and *P27* are presented in graphs of their fold change in comparison to the uninjured control. The levels of expression at 1, 3, 7, and 14 days post spinal cord injury with three treatments of placebo, low dose, and high dose of XPO are compared. These three groups are referred to as group 1, group 2, and group 3. As further experiments are still taking place, I am not yet unblinded to which of the three treatment groups is which.

When a two-way ANOVA was run to compare the expression of *Yap, Taz, Pdgfrb,* and *P27* according to the factors of treatment and time. It found a significant effect of time ($F(3.822\ 35.67) = 25.21$, $p < 0.0001$), but no significant effect of treatment ($F(2, 140) = 2.892$, $p = 0.0588$). To find where the differences lay I ran a one-way ANOVA and used a Bonferroni post-hoc analysis.

Over time after injury, from day 1 to 14 I observed an increase in levels of *Yap* expression in comparison to uninjured levels. There was no significant effect of time ($F(3,8) = 2.698$, $p = 0.1163$) and no significant effect of treatment ($F(2,9) = 0.3492$, $p = 0.7144$). At 1-day post-injury, groups 1, 2, and 3 all experienced increased expression levels in comparison to the control group. Groups 3 and 2 were slightly higher than group 1. At 3 days post-injury, groups 1, 2, and 3 all experienced increased expression levels in comparison to the control group. Group 3 was slightly higher than group 1. At 7 days post-injury, groups 1, 2, and 3 all experienced increased expression levels in comparison to the control group. Groups 1 and 2 were slightly higher than group 3. At 14 days post-injury, groups 1, 2, and 3 all experienced increased expression levels in comparison to the control group. There was no significant difference between the expression level of the different groups at any time points. Group 1 was increased from control group levels at days 1 and 3, and then experienced a peak of a fold change of 1.65 at 7 days post-injury before decreasing slightly at day 14. Expression levels remained above the baseline of the uninjured expression at all timepoints, showing an increase from uninjured expression levels. Group 2 was increased from control group levels at days 1 and 3, and also peaked at 7 dpi with a fold change of 1.41 before decreasing slightly at day 14. Expression levels remained above baseline at all timepoints. Group 3 showed an increase in expression compared to the uninjured group at all timepoints, but only experienced slight variation over time, peaking with a 1.31-fold change at day 3.

Over time after injury, from day 1 to 14, levels of *Taz* both decreased and remained steady in comparison to the uninjured control group. There was no significant effect of time ($F(3,8) = 3.185$, $p = 0.0845$) and no significant effect of treatment ($F(2,9) = 0.2112$, $p = 0.8135$). At 1-day post-injury, there was a decrease in expression level of group 1 while levels in groups 2 and 3 remained constant in comparison to the control group. At 3 days post-injury, groups 1, 2, and 3 all experienced a decrease in expression levels from those of the control group. At 7 days post-injury, groups 1 and 2 returned to within baseline levels, while levels in group 3 remained below that of the control group. At 14 days post-injury, groups 1, 2, and 3 all remained within baseline levels, not varying significantly from that of the control group. group 1 decreased in expression at days 1 and 3, with its lowest level of a -0.79-fold change from uninjured at day 3, before returning to baseline at days 7 and 14. Group 2 fluctuated slightly over time,

remaining at baseline at day 1, decreasing most at day 3 with a fold change of -0.26, returning to baseline at day 7, and decreasing to slightly below baseline again at day 14. The expression of group 3 remained at baseline at day 1 before decreasing with a fold change of -0.21 at days 3 and 7 and returning to baseline at day 14.

Over time after injury, from day 1 to 14 I observed a both increased and decreased expression of *P27* in comparison to uninjured levels. There was a significant effect of time ($F(3,8) = 0.0044$, $p = 0.9996$) and no significant effect of treatment ($F(2,9) = 2.310$, $p = 0.1550$). At 1-day post-injury, expression levels of groups 1, 2, and 3 experienced a decrease in expression levels. There were no significant differences between the expression levels of the different groups. At 3 days post-injury, groups 1, 2, and 3 experienced a decrease in expression levels compared to the control group. There were no significant differences between the expression levels of the different groups. There was a notable difference in the expression levels of group 1 in comparison to the other groups at days 7 and 14. At 7 days post-injury, group 1 experienced an increase beyond the levels of the control group. Expression levels of group 2 and group 3 decreased from the baseline, while group 1 was slightly higher ($p = 0.1550$). At 14 days post-injury, group 1 expression levels continued to be higher than the levels of the control group. Expression levels of group 2 and group 3 remained less than the baseline. There was a difference ($p = 0.1550$) between the groups of expression levels, as group 1 was higher than that of groups 2 and 3. Expression levels of group 1 were at baseline 1-day post injury and decreased slightly below at day 3 with a fold change of -1.0. At days 7 and 14 group 1 peaked, rising significantly above the levels of the control group. The peak at day 14 had a fold change of 2.3. Expression levels of group 2 were below control levels at day 1, at baseline at day 3, and below baseline at 7 and 14 dpi, reaching its lowest levels at day 7 with a fold change of -1.3. Expression levels of group 3 were slightly below control levels at days 1 and 3, and dipped even lower at days 7 and 14. On day 14 there was a fold change of -1.3.

Over time after injury, from day 1 to 14 I observed an increase in levels of *Pdgfrb* expression in comparison to uninjured levels. There was no significant effect of time ($F(3,8) = 1.996$, $p = 0.1933$) and no significant effect of treatment ($F(2,9) = 0.5259$, $p = 0.6081$). At 1-day post-injury, expression levels of group 1 remained below those of the control group while levels in groups 2 and 3 rose in comparison to the control group. At 3 days post-injury, groups 1, 2, and 3 all experienced an increase in expression levels from those of the control group. There was a small difference ($p = 0.6081$) between the groups, as group 1 increased more than in groups 2 and 3. At 7 days post-injury, groups 1, 2, and 3 all had expression levels above the control group, and there was not a significant difference between groups. At 14 days post-injury all the groups had extreme variability. Group 1 began at 1-day post-injury within baseline levels before increasing at days 3, 7, and 14 to above the levels of the control group. The peak was at 14 days post-injury with a fold change of 3.3, however there was no significant difference between expression levels of group 1 at days 3, 7, and 14. Group 2 was slightly increased from baseline at day 1, experienced a further increase at days 3 and 7, and was within baseline levels again at day 14. It peaked at day 7 with a fold change of 2.8. Expression levels of group 3 remained increased from the control group at days 1, 3, 7, and 14, peaking at day 7 with a fold change of 2.9.

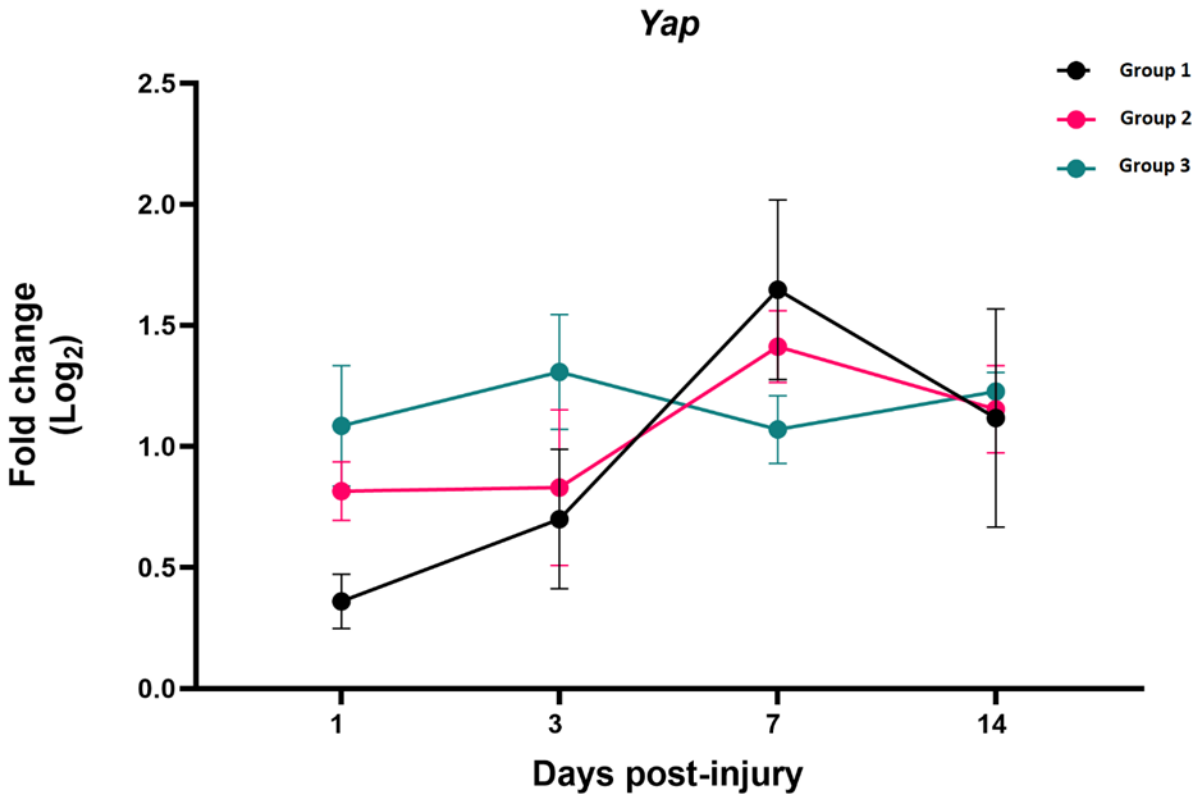

Fig. 1: The fold change in levels of *Yap* expression based on the different conditions of placebo, low dose, and high dose, and based on days post-injury compared to the uninjured control.

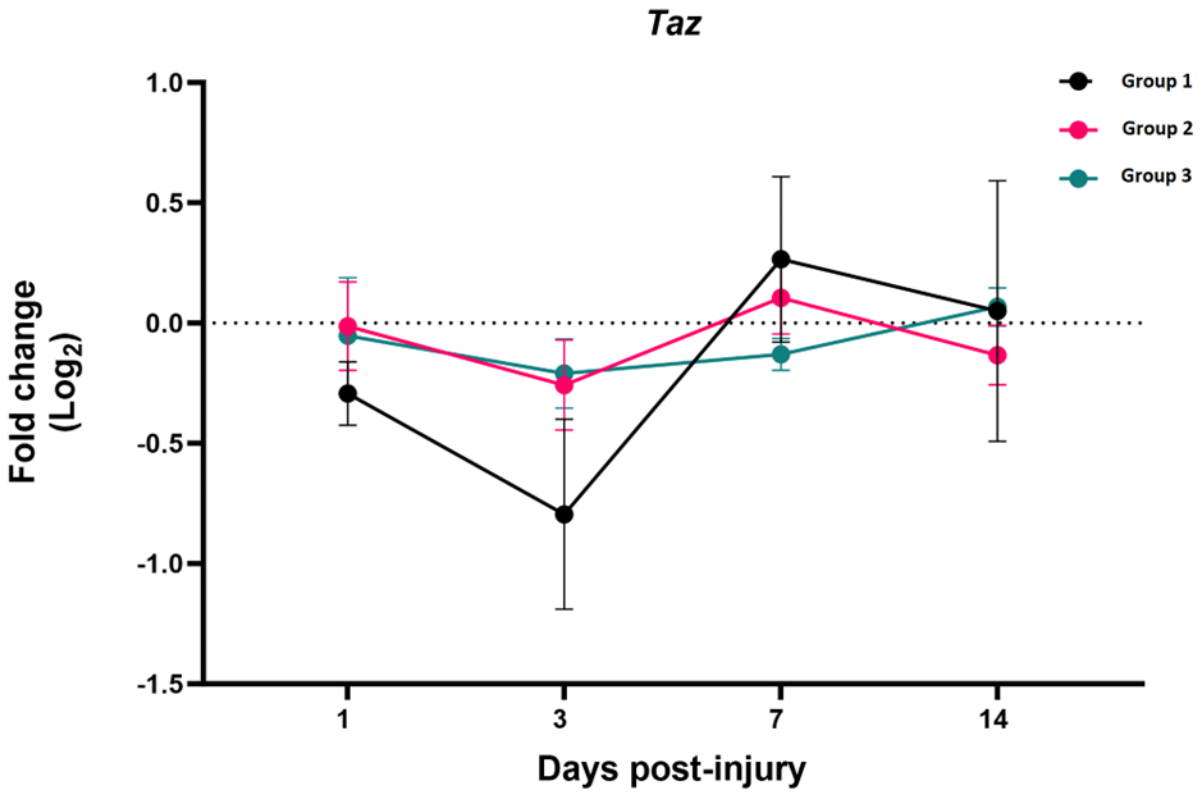

Fig. 2: The fold change in levels of *Taz* expression based on the different conditions of placebo, low dose, and high dose, and based on days post-injury compared to the uninjured control.

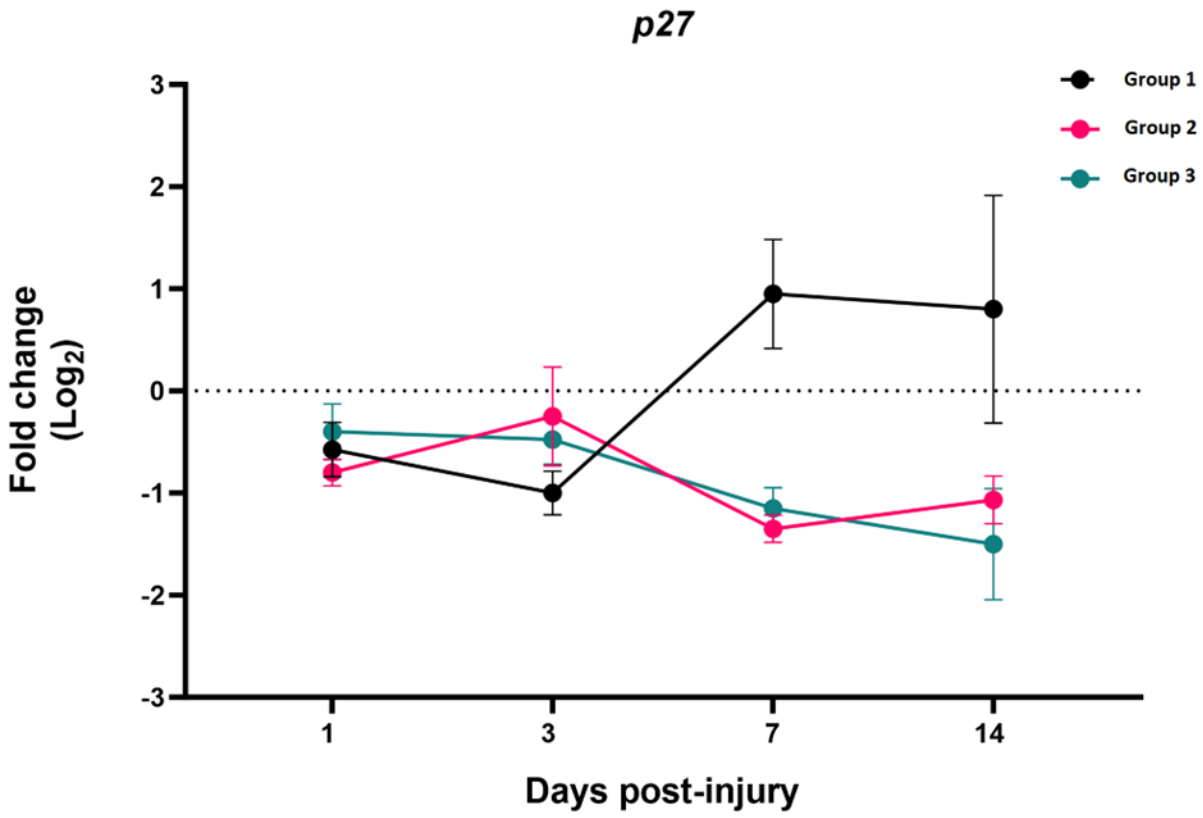

Fig. 3: The fold change in levels of *P27* expression based on the different conditions of placebo, low dose, and high dose, and based on days post-injury compared to the uninjured control.

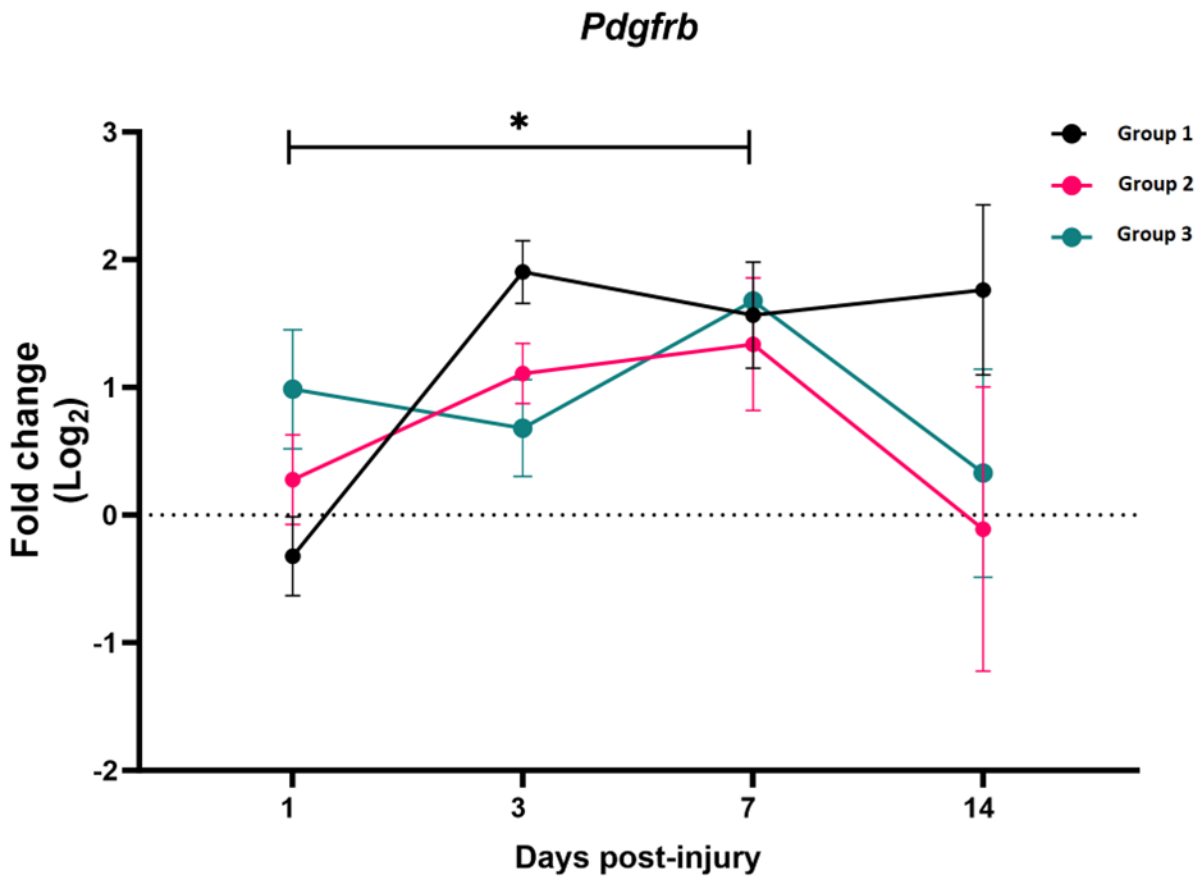

Fig. 4: The fold change in levels of *Pdgfrb* expression based on the different conditions of placebo, low dose, and high dose, and based on days post-injury compared to the uninjured control.

IV. Discussion:

The glial and fibrotic scars that form after spinal cord injury both impede axonal regeneration and have protective effects. The formation of these scars involves several proteins that are effected by XPO nuclear export. In this study the effect of inhibiting XPO on the expression levels of *Yap*, *Taz*, *P27*, and *Pdgfrb*, which are linked to scar formation, is explored. At an mRNA level, no differences in the expression these target genes were detected. Despite a lack of statistically significant differences between the expression levels of the studied genes between the treatment groups, a minor difference was seen in group 1 for *p27*. *P27* levels were lower than the control group at all timepoints in groups 3 and 2, while in group 1 the expression levels rose by days 7 and 14. At days 7 and 14 group 1 was higher than groups 2 and 3. The genes had no true trends between groups. *Yap* expression levels were continually raised above those of the uninjured control group. *Taz* expression levels varied from below and similar to those of the uninjured control group. *Pdgfrb* expression levels were mainly above and within range of those of the control group.

My hypothesis was that there would be changes in expression levels due to treatment in all the genes studied, showing a change in the glial and fibrotic scar. However, the changes seen were mainly

minor and not statistically significant. *Yap* and *Taz*, both important in glial and fibrotic scar formation, experienced extremely slight changes in expression when treatment was given. This could show that inhibiting XPO does not affect the glial and fibrotic scar through mechanisms of changing *Yap* and *Taz* expression, but rather by allowing their continual function. There could be changes in protein levels rather than mRNA levels. YAP and TAZ proteins are continually functioning they will lead to an increase in astrocyte proliferation and fibrosis. This would increase glial and fibrotic scarring. *P27* experienced an slight increase in expression with group 1 treatment at later time points, which, while not statistically significant, could point to an effect of the treatment. It was expected that *P27* would decrease in expression with treatment as a result of increased YAP function. If group 1, which has higher levels of *P27* at days 7 and 14, is the placebo, then the treatment may cause a decrease in *P27* expression levels. Decreased *P27* levels would point to changes in the amount of YAP functioning and cause increased astrocyte proliferation. *Pdgfrb*, a gene involved in fibrosis, similarly experienced such slight changes that do not seem to show a consistent pattern or effect of treatment. Overall, these results could point to a possible lack of a major change in the fibrotic scar and glial scar or simply a lack of change in the specific genes studied. Additionally, XPO inhibition could affect protein levels instead of mRNA levels.

The high standard error of the mean seen between our results, the high biological variability (specifically at day 7), and the low power effect can affect the data gathered. Future experiments should achieve more reliable data to strengthen or disprove the conclusions made. Completing the experiment with more animals will allow for an increased power effect leading to less variable and more robust data, which will allow for more solid conclusions.

V. Conclusion:

Slight variation in expression levels of *Yap, Taz, P27,* and *Pdgfrb* were seen, with no statistical significance. Despite the lack of statistical significance, the slight differences in *P27* expressions could point to potential effects of inhibiting XPO on scarring after spinal cord injury. The decrease in expression of *P27* with groups 2 and 3 in comparison to group 1 could point to the increased functioning of YAP. This potential increased function of YAP and TAZ proteins would lead to increased fibrosis and glial scarring, affecting recovery. The limitations of this experiment, as previously discussed, lead to a need for further research to be conducted. Using more animals to increase the significance of the data would be helpful. An experiment in which both expression levels and levels of the proteins themselves were studied could also provide more clarity. More definite conclusions about the effect of inhibiting XPO on genes related to scarring after spinal cord injury remain to be made.

VI. References:

Spinal cord injury. (2013, November 19). Spinal Cord Injury. https://www.who.int/news-room/fact-sheets/detail/spinal-cord-injury

Ayazi, M., Zivkovic, S., Hammel, G., Stefanovic, B., & Ren, Y. (2022, August 2). Fibrotic Scar in CNS Injuries: From the Cellular Origins of Fibroblasts to the Molecular Processes of Fibrotic Scar Formation. *Cells*, *11*(15), 2371. https://doi.org/10.3390/cells11152371

Wanner, I. B., Anderson, M. A., Song, B., Levine, J., Fernandez, A., Gray-Thompson, Z., Ao, Y., & Sofroniew, M. V. (2013, July 31). Glial Scar Borders Are Formed by Newly Proliferated, Elongated Astrocytes That Interact to Corral Inflammatory and Fibrotic Cells via STAT3-Dependent Mechanisms

after Spinal Cord Injury. *Journal of Neuroscience*, *33*(31), 12870–12886. https://doi.org/10.1523/jneurosci.2121-13.2013

Zhang, W., Jia, M., Lian, J., Lu, S., Zhou, J., Fan, Z., Zhu, Z., He, Y., Huang, C., Zhu, M., Wang, J., Wang, Y., Huang, Z., & Teng, H. (2023, April 10). Inhibition of TANK-binding kinase1 attenuates the astrocyte-mediated neuroinflammatory response through YAP signaling after spinal cord injury. *CNS Neuroscience & Therapeutics*. https://doi.org/10.1111/cns.14170

Hellenbrand, D. J., Quinn, C. M., Piper, Z. J., Morehouse, C. N., Fixel, J. A., & Hanna, A. S. (2021, December 7). Inflammation after spinal cord injury: a review of the critical timeline of signaling cues and cellular infiltration. *Journal of Neuroinflammation*, *18*(1). https://doi.org/10.1186/s12974-021-02337-2

Parikh, K., Cang, S., Sekhri, A., & Liu, D. (2014, October 15). Selective inhibitors of nuclear export (SINE)– a novel class of anti-cancer agents. *Journal of Hematology & Oncology*, *7*(1). https://doi.org/10.1186/s13045-014-0078-0

Hutten, S., & Kehlenbach, R. H. (2007, April). CRM1-mediated nuclear export: to the pore and beyond. *Trends in Cell Biology*, *17*(4), 193–201. https://doi.org/10.1016/j.tcb.2007.02.003

Xie, C., Shen, X., Xu, X., Liu, H., Li, F., Lu, S., Gao, Z., Zhang, J., Wu, Q., Yang, D., Bao, X., Zhang, F., Wu, S., Lv, Z., Zhu, M., Xu, D., Wang, P., Cao, L., Wang, W., . . . Huang, Z. (2020, February 17). Astrocytic YAP Promotes the Formation of Glia Scars and Neural Regeneration after Spinal Cord Injury. *The Journal of Neuroscience*, *40*(13), 2644–2662. https://doi.org/10.1523/jneurosci.2229-19.2020

Totaro, A., Panciera, T., & Piccolo, S. (2018, July 26). YAP/TAZ upstream signals and downstream responses. *Nature Cell Biology*, *20*(8), 888–899. https://doi.org/10.1038/s41556-018-0142-z

Meng, Z., Moroishi, T., & Guan, K. L. (2016, January 1). Mechanisms of Hippo pathway regulation. *Genes & Development*, *30*(1), 1–17. https://doi.org/10.1101/gad.274027.115

Hoxha, S., Shepard, A., Troutman, S., Diao, H., Doherty, J. R., Janiszewska, M., Witwicki, R. M., Pipkin, M. E., Ja, W. W., Kareta, M. S., & Kissil, J. L. (2020, June 15). YAP-Mediated Recruitment of YY1 and EZH2 Represses Transcription of Key Cell-Cycle Regulators. *Cancer Research*, *80*(12), 2512–2522. https://doi.org/10.1158/0008-5472.can-19-2415

Spinal Cord Injury. (2023, January 20). National Institute of Neurological Disorders and Stroke. https://www.ninds.nih.gov/health-information/disorders/spinal-cord-injury

Yao, F., Luo, Y., Liu, Y. C., Chen, Y. H., Li, Y. T., Hu, X. Y., You, X. Y., Yu, S. S., Li, Z. Y., Chen, L., Tian, D. S., Zheng, M. G., Cheng, L., & Jing, J. H. (2022, September 26). Imatinib inhibits pericyte-fibroblast transition and inflammation and promotes axon regeneration by blocking the PDGF-BB/PDGFRβ pathway in spinal cord injury. *Inflammation and Regeneration*, *42*(1). https://doi.org/10.1186/s41232-022-00223-9

Li, Z., Yu, S., Hu, X., Li, Y., You, X., Tian, D., Cheng, L., Zheng, M., & Jing, J. (2021, August 26). Fibrotic Scar After Spinal Cord Injury: Crosstalk With Other Cells, Cellular Origin, Function, and Mechanism. *Frontiers in Cellular Neuroscience*, *15*. https://doi.org/10.3389/fncel.2021.720938

Shi, Z., Yuan, S., Shi, L., Li, J., Ning, G., Kong, X., & Feng, S. (2021, January 27). Programmed cell death in spinal cord injury pathogenesis and therapy. *Cell Proliferation*, *54*(3). https://doi.org/10.1111/cpr.12992

Ishii, Y., Hamashima, T., Yamamoto, S., & Sasahara, M. (2017, April 10). Pathogenetic significance and possibility as a therapeutic target of platelet derived growth factor. *Pathology International*, *67*(5), 235–246. https://doi.org/10.1111/pin.12530

Funa, K., & Sasahara, M. (2013, June 15). The Roles of PDGF in Development and During Neurogenesis in the Normal and Diseased Nervous System. *Journal of Neuroimmune Pharmacology*, *9*(2), 168–181. https://doi.org/10.1007/s11481-013-9479-z

Perez-Gianmarco, L., & Kukley, M. (2023, July 13). Understanding the Role of the Glial Scar through the Depletion of Glial Cells after Spinal Cord Injury. *Cells*, *12*(14), 1842. https://doi.org/10.3390/cells12141842

Talbott, H. E., Mascharak, S., Griffin, M., Wan, D. C., & Longaker, M. T. (2022, August). Wound healing, fibroblast heterogeneity, and fibrosis. *Cell Stem Cell*, *29*(8), 1161–1180. https://doi.org/10.1016/j.stem.2022.07.006

Mia, M. M., & Singh, M. K. (2022, June 29). New Insights into Hippo/YAP Signaling in Fibrotic Diseases. *Cells*, *11*(13), 2065. https://doi.org/10.3390/cells11132065

KEGG PATHWAY: Hippo signaling pathway - Reference pathway. (n.d.). KEGG PATHWAY: Hippo Signaling Pathway - Reference Pathway. https://www.kegg.jp/pathway/map=map04390&keyword=yap

Kjell, J., & Olson, L. (2016, October 1). Rat models of spinal cord injury: from pathology to potential therapies. *Disease Models & Mechanisms*, *9*(10), 1125–1137. https://doi.org/10.1242/dmm.025833